Electronic Supplementary Information

Experimental Section

Materials: Sodium nitrate (NaNO$_3$, 99.9%), sodium nitrite (NaNO$_2$, 99.0%), ammonium chloride (NH$_4$Cl), sodium hydroxide (NaOH), ethanol (C$_2$H$_6$O, 99.9%), sodium salicylate (C$_7$H$_5$NaO$_3$), trisodium citrate dihydrate (C$_6$H$_5$Na$_3$O$_7$·2H$_2$O), p-dimethylaminobenzaldehyde (C$_9$H$_{11}$NO), sodium nitroferricyanide dihydrate (C$_5$FeN$_6$Na$_2$O·2H$_2$O), and sodium hypochlorite solution (NaClO) were purchased from Aladdin Co., Ltd. (Shanghai, China). Sulfuric acid (H$_2$SO$_4$), hydrogen peroxide (H$_2$O$_2$), hydrochloric acid (HCl), hydrazine monohydrate (N$_2$H$_4$·H$_2$O), and ethylalcohol (C$_2$H$_5$OH) were bought from Beijing Chemical Corporation. (China). Iron nitrate nonahydrate (Fe(NO$_3$)$_3$·9H$_2$O) were purchased from Chengdu Kelong Chemical Regent Co. Ltd. Ti plate (thickness is 0.2 mm) was purchased from Qingyuan Metal Materials Co., Ltd (Xingtai, China) and treated with 3 M HCl for 30 min before hydrothermal reaction. All reagents used in this work were analytical grade without further purification.

Preparation of Fe-TiO$_2$/TP: Firstly, Ti plate (2.0 × 3.0 cm^2) was cleaned by ultrasonication in acetone, ethanol, and water for 15 min, respectively. Then, the Ti plate was put into a 50 mL Teflon-lined autoclave containing 35 mL of 5 M NaOH solution. After the autoclave was kept in an electric oven at 180 °C for 24 h. After the autoclave was cooled down naturally to room temperature, the sample was moved out, washed with deionized water and ethanol several times and dried at 60 °C for 30 min. Then the obtained Na-titanate/TP was immersed in 0.25 M Fe(NO$_3$)$_3$ for 1 h to exchange Na$^+$ with Fe^{3+}. The resulting Fe-titanate/TP was rinsed with deionized water and ethanol several times and dried at 60 °C for 30 min. Subsequently, Fe-titanate/TP was annealed in a tube furnace at 500 °C under an Ar atmosphere for 2 h. After cooling to room temperature, Fe-TiO$_2$/TP was finally obtained. As a control, TiO$_2$/TP was prepared by the same fabrication process of Fe-TiO$_2$/TP except for immersing the Na-

titanate/TP into 1 M HCl solution to exchange Na^+ with H^+.

Characterizations: XRD data was acquired from a LabX XRD-6100 X-ray diffractometer with a Cu Kα radiation (40 kV, 30 mA) of wavelength 0.154 nm (SHIMADZU, Japan). SEM images were collected on a GeminiSEM 300 scanning electron microscope (ZEISS, Germany) at an accelerating voltage of 5 kV. TEM images were acquired on a HITACHI H-8100 electron microscope (Hitachi, Tokyo, Japan) operated at 200 kV. XPS measurements were performed on an ESCALABMK II X-ray photoelectron spectrometer using Mg as the exciting source. The absorbance data of spectrophotometer was measured on UV-Vis spectrophotometer (SHIMADZU UV-2700). Gaseous products from nitrate reduction reaction were determined by gas chromatography with SHIMADZU GC-2014 gas chromatograph. ^1H NMR spectra were collected on Varian VNMRS 600 MHz (the USA).

Electrochemical measurements: All electrochemical measurements were carried on the CHI660E electrochemical workstation (Shanghai, Chenhua) using a standard three-electrode setup. Electrolyte solution was Ar-saturated of 0.1 M NaOH with 0.1 M NO_3^-, using Fe-TiO_2/TP, TiO_2/TP, or TP as working electrode, a graphite rod as the counter electrode, and a Hg/HgO as the reference electrode. We use an H-type electrolytic cell separated by a Nafion 117 membrane which was protonated by boiling in ultrapure water, H_2O_2 (5%) aqueous solution and 0.5 M H_2SO_4 at 80 °C for another 2 h, respectively. All the potentials reported in our work were converted to reversible hydrogen electrode via calibration with the following equation: E (RHE) = E (Hg/HgO) + (0.098 + 0.0591 × pH) V and the presented current density was normalized to the geometric surface area.

Determination of NH_3: The NH_3 concentration in the solution was determined by colorimetry using the indophenol blue method.[1] In detail, 2 mL of the solution after reaction (the obtained electrolyte was diluted 40 times), and 2 mL of 1 M NaOH coloring solution containing 5% salicylic acid and 5% sodium citrate. Then, 1 mL

oxidizing solution of 0.05 M NaClO and 0.2 mL catalyst solution of $C_5FeN_6Na_2O$ (1 wt%) were added to the above solution. After standing in the dark for 2 h, the UV-Vis absorption spectra were measured. The concentration of NH_3 was identified using the absorbance at a wavelength of 655 nm. The concentration-absorbance curve was calibrated using the standard NH_4Cl solution with NH_3 concentrations of 0, 0.2, 0.5, 1.0, 2.0, and 5.0 ppm in 0.1 M NaOH solution. The fitting curve (y = 0.4328 x + 0.0916, R^2 = 0.9998) shows good linear relation of absorbance value with NH_3 concentration.

Determination of N_2H_4: The N_2H_4 was estimated by the Watt and Chrisp method.[2] The color reagent was a solution of 18.15 mg mL^{-1} of $C_9H_{11}NO$ in the mixed solvent of HCl and C_2H_5OH (V/V: 1/10). In detail, 2 mL electrolyte was added into 2 mL color reagent for 15 min under stirring. The absorbance of such solution was measured to quantify the hydrazine yields by the standard curve of hydrazine (y = 0.7013 x + 0.1002, R^2 = 0.9999).

Determination of NO_2^-: The NO_2^- concentration was quantitatively determined by Griess method.[3] Firstly, 1.0 mL of deionized water, 1.0 mL of sample solution, and 2.0 mL of Griess reagent were sequentially added to a 10 mL of centrifuge tube. The absorbance at 540 nm was then measured by a UV-Vis spectrophotometer after 15 min of dark incubation. The concentration-absorption spectra were calibrated using standard $NaNO_2$ solution with different concentration (y = 0.2078 x + 0.0647, R^2 = 0.9997).

Determination of N_2 and H_2: N_2 and H_2 were quantified by GC.

Calculations of the m_{NH3}, FE and NH_3 yield:

The amount of NH_3 (n_{NH3}) was calculated by the following equation:

$$n_{NH3} = [NH_3] \times V$$

FE of NH_3 formation was calculated by the following equation:

$$FE = (8 \times F \times [NH_3] \times V) / (M_{NH3} \times Q) \times 100\%$$

NH_3 yield rate is calculated using the following equation:

$$NH_3 \text{ yield} = ([NH_3] \times V) / (M_{NH3} \times t \times A)$$

Where F is the Faradic constant (96485 C mol^{-1}), [NH$_3$] is the NH$_3$ concentration, V is the volume of electrolyte in the anode compartment (40 mL), M$_{NH3}$ is the molar mass of NH$_3$ molecule, Q is the total quantity of applied electricity; t is the electrolysis time (1 h) and A is the geometric area of working electrode (0.5 × 0.5 cm^2).

DFT calculation: All DFT calculations were conducted by plane-wave DFT implemented in the Vienna *Ab initio* Simulation Package (VASP). Potentials constructed with the full potential projector augmented wave (PAW) method were used for the elemental constituents. The exchange correlation was treated with the generalized gradient approximation (GGA) Perdew-Burke-Ernzerhof (PBE) functional.[4] Spin polarization was also included. A (3 × 1) unit cell of TiO$_2$ (101) slab was constructed for the DFT calculation.[5] The cell length was 10.45 Å × 11.35 Å for x and y direction. 2 layers of TiO$_2$ were constructed along the z direction, with a vacuum layer of 20 Å. In each calculation, 500 eV cutoff energy and 2 × 2 × 1 K-mesh were chosen to achieve a convergence of 2 meV/atom. The convergence criteria were set to be the energy of 10^{-6} eV/atom and the force of 0.2 eV/nm for the electronic and ionic steps in relaxation, respectively. In the relaxation, the bottom layer was fixed while the upper layer was allowed to move. The Gibbs free energy of each structure was the DFT calculated energy added by the Gibbs free energy term. The former can be directly obtained from DFT while the latter was obtained by calculating the vibration frequency.
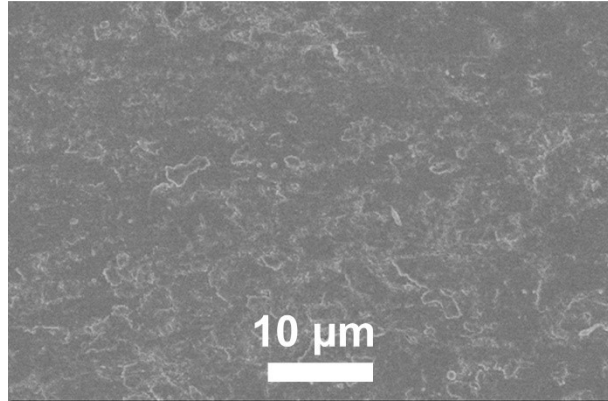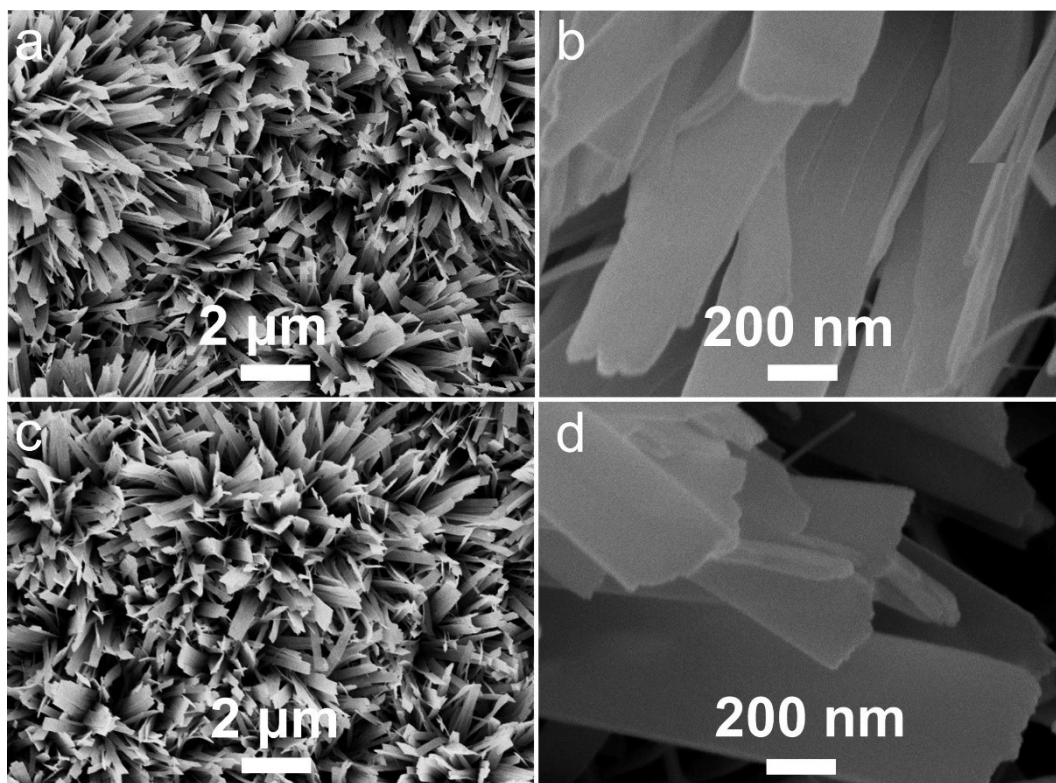
Fig. S1. SEM image of bare TP.

Fig. S2. (a) Low- and (b) high-magnification SEM images of Na-titanate/TP. (c) Low- and (d) high-magnification SEM images of Fe-titanate/TP.
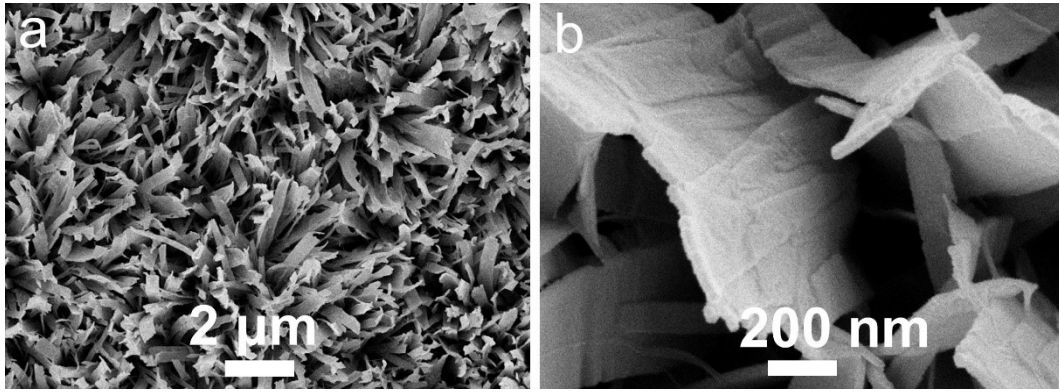
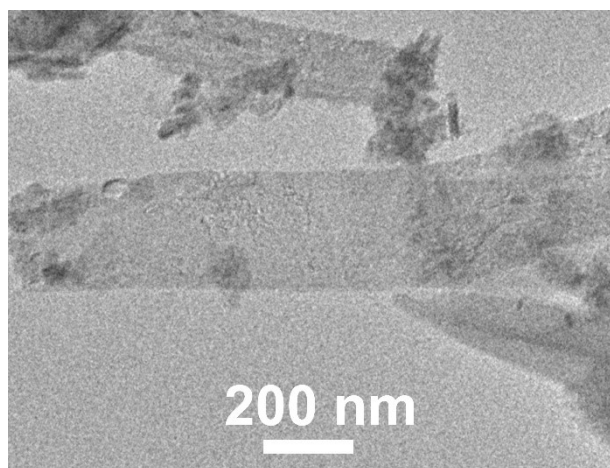**Fig. S3.** (a) Low- and (b) high-magnification SEM images of TiO$_2$/TP.
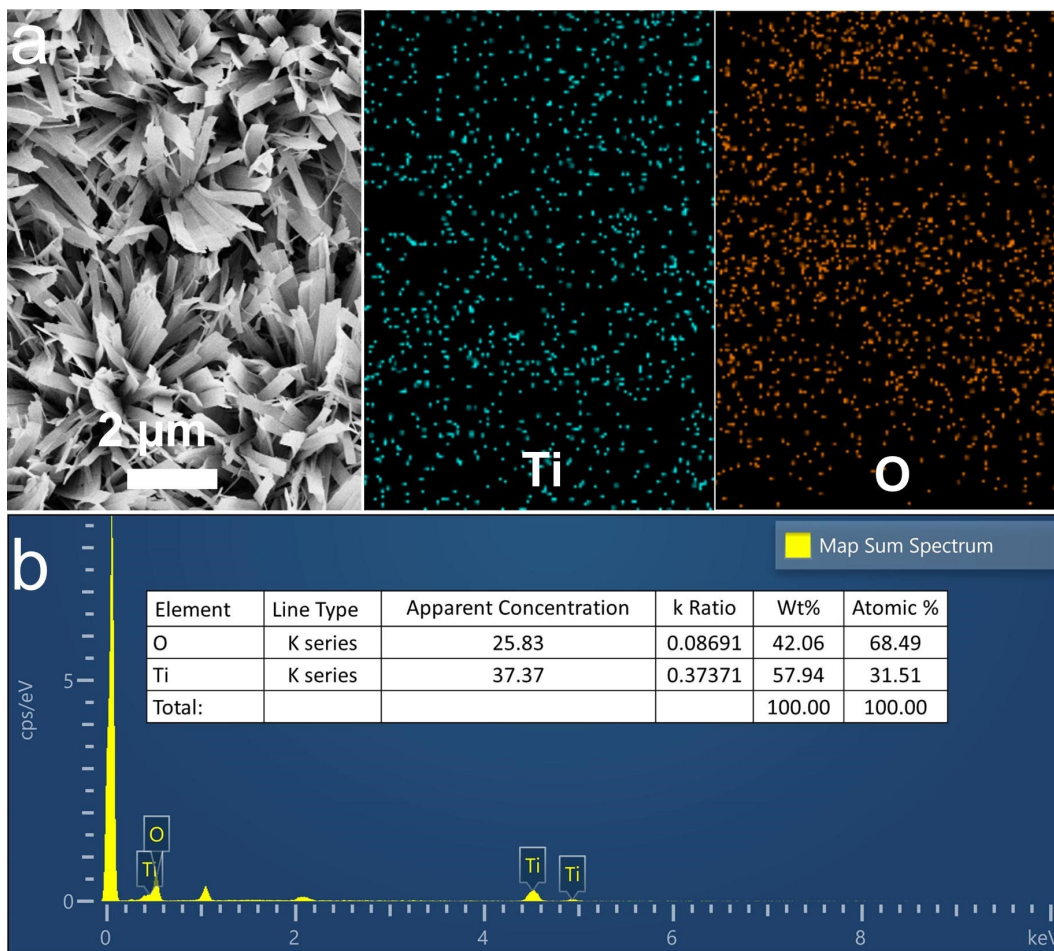
Fig. S4. TEM image of TiO$_2$ nanoribbon.

Element	Line Type	Apparent Concentration	k Ratio	Wt%	Atomic %
O	K series	25.83	0.08691	42.06	68.49
Ti	K series	37.37	0.37371	57.94	31.51
Total:				100.00	100.00

Fig. S5. (a) SEM and corresponding EDX mapping images of Ti and O for TiO$_2$/TP. (b) EDX spectrum of TiO$_2$/TP.

Element	Line Type	Apparent Concentration	k Ratio	Wt%	Atomic %
O	K series	16.07	0.05407	34.52	61.94
Ti	K series	42.73	0.42729	51.73	31.00
Fe	K series	10.63	0.10632	13.74	7.06
Total:				100.00	100.00
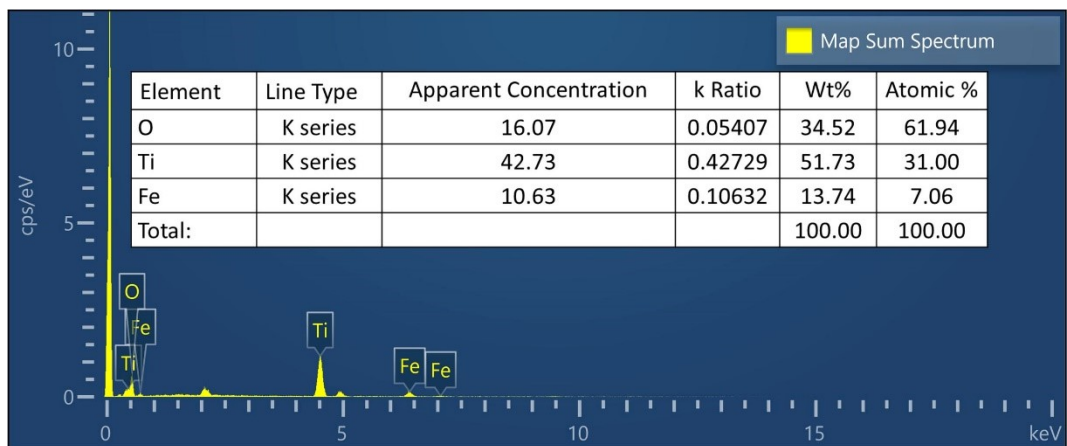
Fig. S6. EDX spectrum of Fe-TiO$_2$/TP.
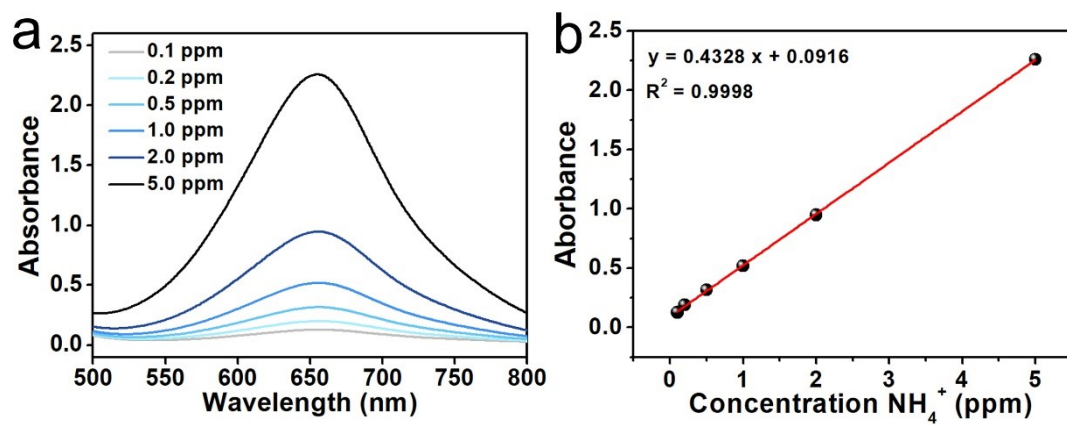
Fig. S7. (a) UV-Vis absorption spectra and (b) corresponding calibration curve for calculation of NH_4^+ concentration.
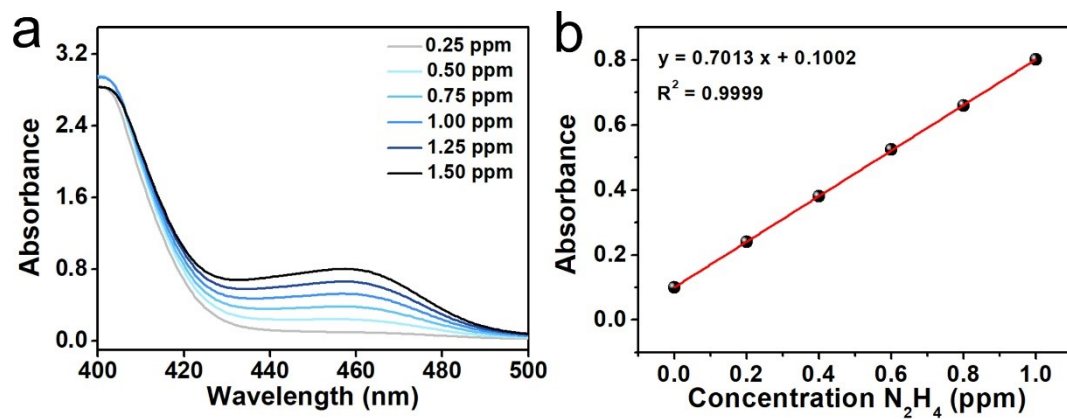
Fig. S8. (a) UV-Vis absorption spectra and (b) corresponding calibration curve for calculation of N_2H_4 concentration.
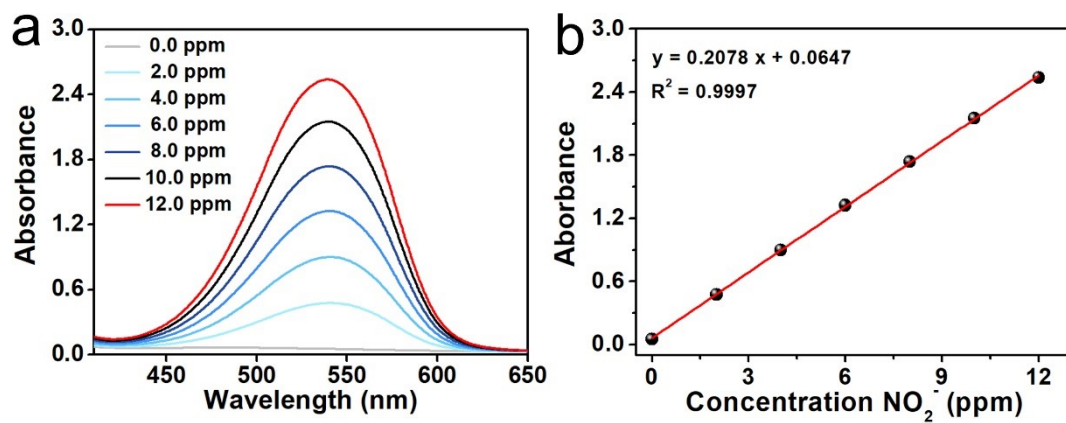
Fig. S9. (a) UV-Vis absorption spectra of various NO_2^- concentrations after incubated for 10 min at room temperature. (b) Calibration curve used for quantification of NO_2^- concentration.
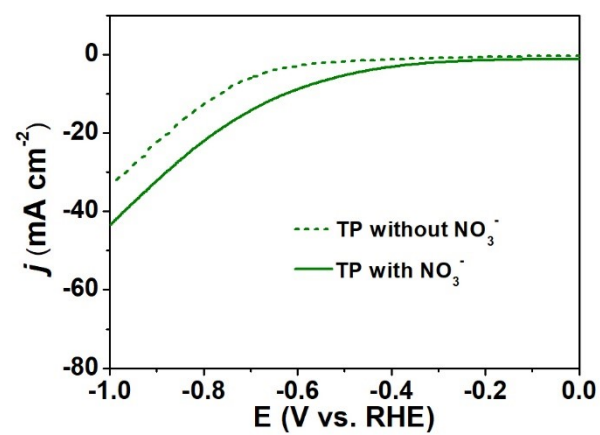
Fig. S10. LSV curves of bare TP in 0.1 M NaOH with/without 0.1 M NaNO$_3$.
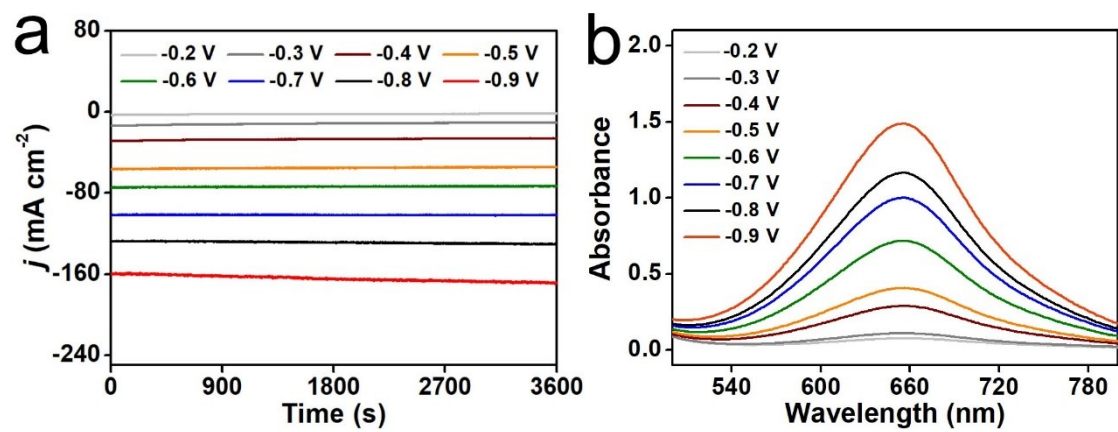
Fig. S11. (a) Chronoamperometry curves and (b) corresponding UV-Vis spectra at a potential range from −0.2 V to −0.9 V.
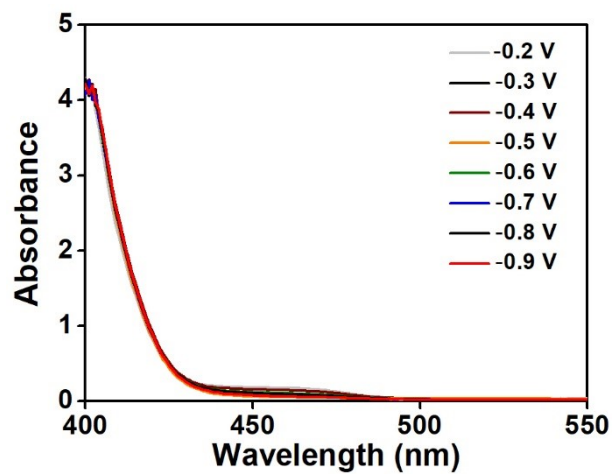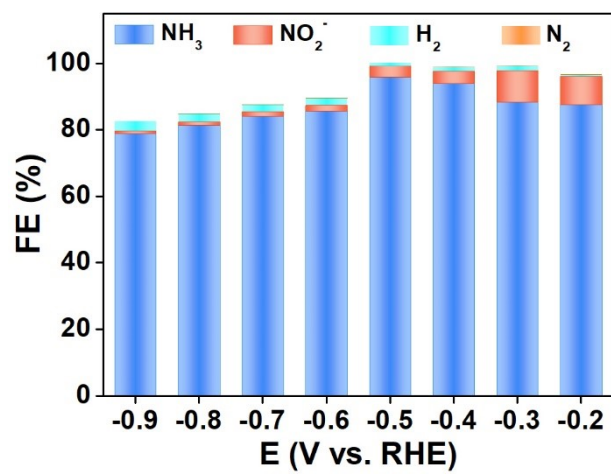
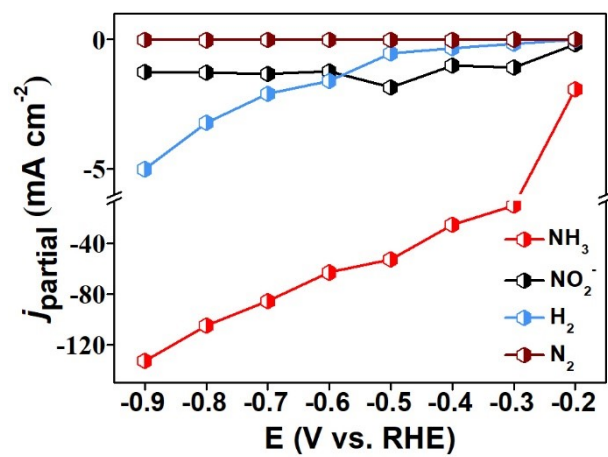**Fig. S12.** UV-Vis absorption spectra of N_2H_4 detection.

Fig. S13. FEs of NH_3, NO_2^-, N_2, and H_2.

Fig. S14. Partial current densities of NH_3, NO_2^-, H_2, and N_2.
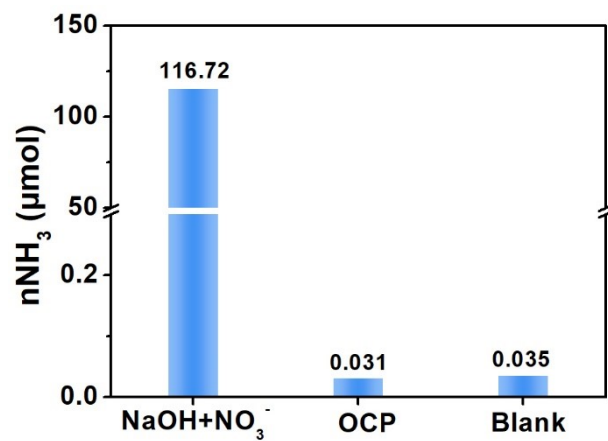
Fig. S15. NO_3^-RR performance of Fe-TiO_2/TP under different test conditions.
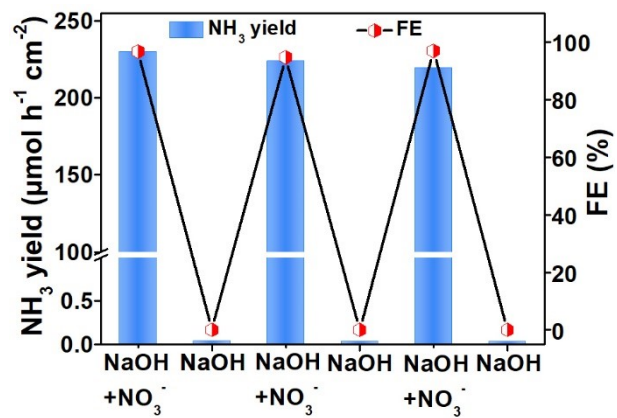
Fig. S16. NH$_3$ yields and FEs during the alternate cycle tests in NO$_3^-$-containing and NO$_3^-$-free 0.1 M NaOH at −0.5 V.
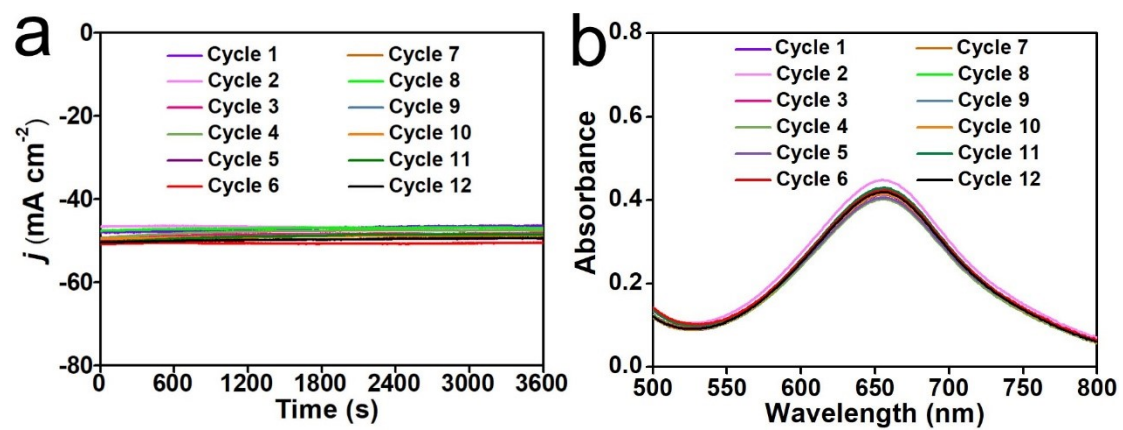
Fig. S17. (a) Chronoamperometry curves and (b) corresponding UV-Vis spectra of Fe-TiO$_2$/TP for generated NH$_3$ during recycling tests at –0.5 V.
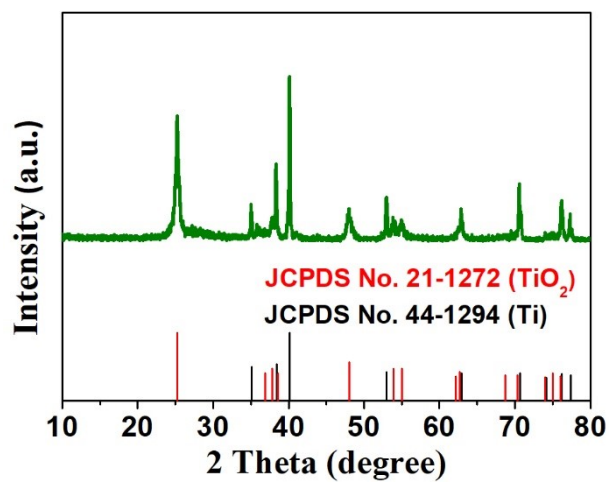
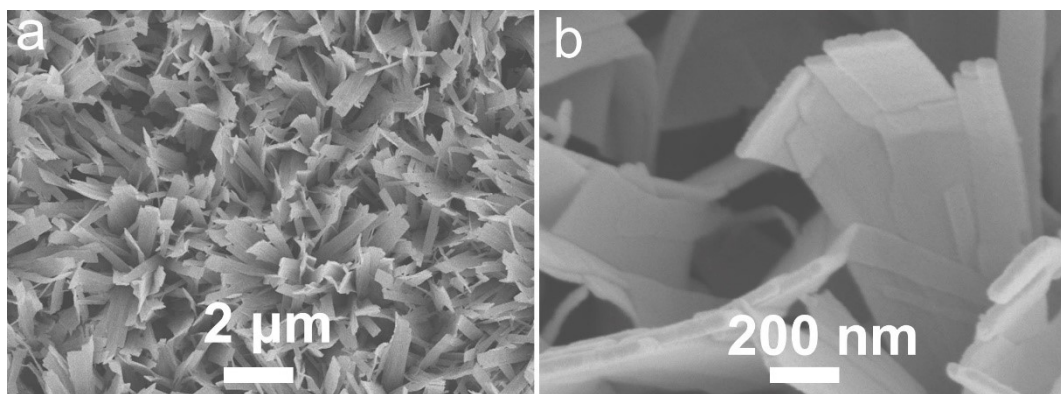**Fig. S18.** XRD pattern of Fe-TiO$_2$/TP after stability test.

Fig. S19. (a) Low- and (b) high-magnification SEM images for Fe-TiO$_2$/TP after stability test.
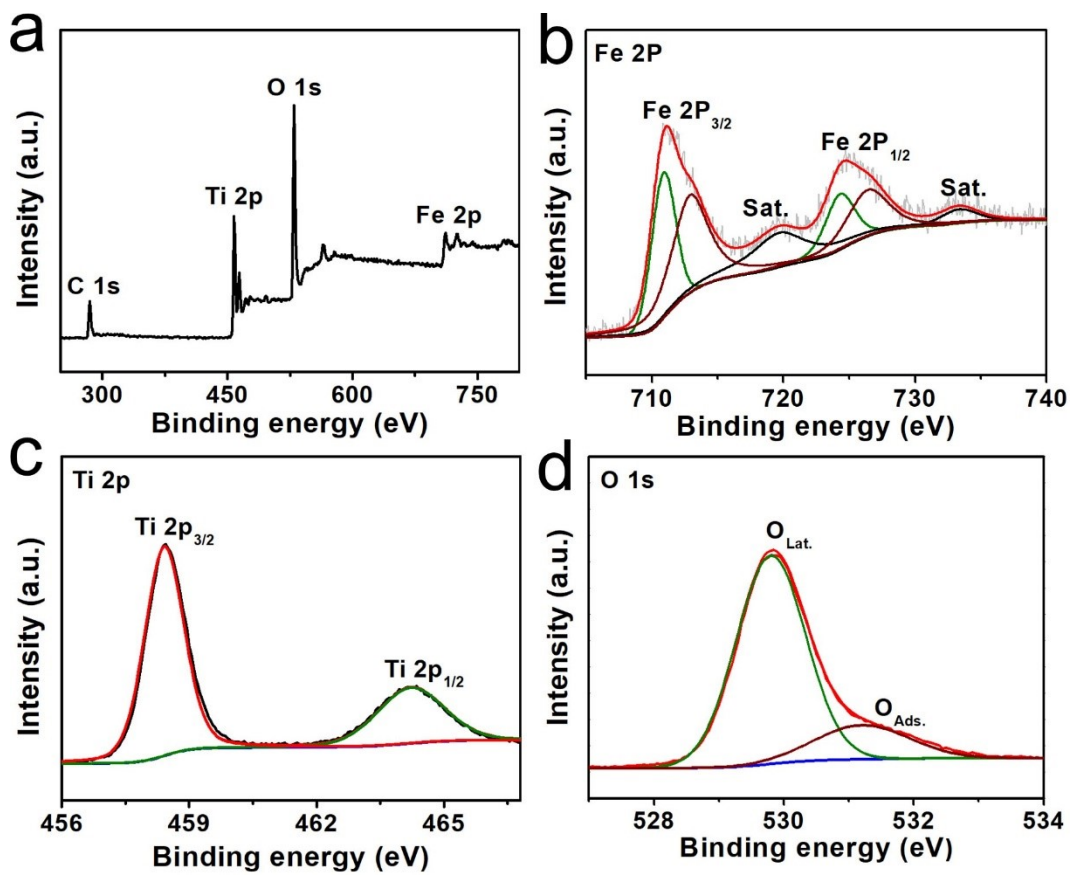
Fig. S20. (a) XPS survey spectrum. XPS spectra of (b) Fe 2p, (c) Ti 2p, and (d) O 1s regions for Fe-TiO$_2$/TP after stability test.
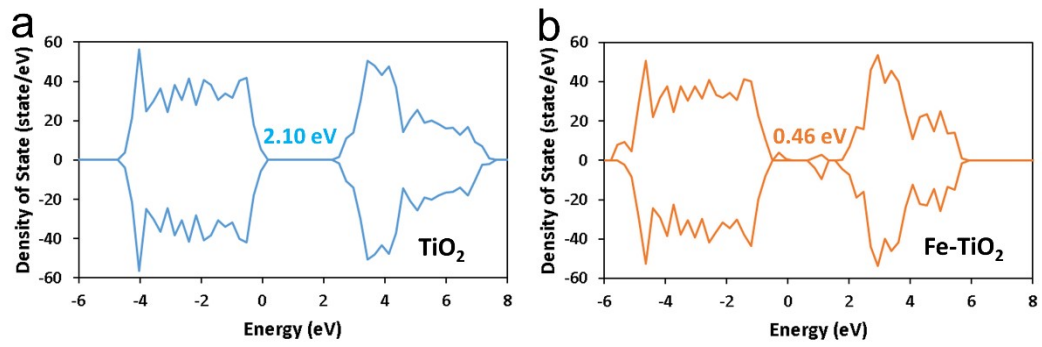
Fig. S21. Electronic density of states of (a) TiO_2 and (b) Fe-TiO_2.

Table S1. Comparison of the catalytic performance of Fe-TiO$_2$/TP with other reported NO$_3^-$RR electrocatalysts.

Catalyst	Electrolyte	NH$_3$ yield (μmol h^{-1} cm^{-2})	FE (%)	Ref.
Fe-TiO$_2$/TP	0.1 M NaOH (0.1 M NaNO$_3$)	970.1	95.9	This work
TiO$_{2-x}$	0.5 M Na$_2$SO$_4$ (50 ppm NaNO$_3$)	45.0	85.0	6
Pd/TiO$_2$	0.5 M NaOH (0.25 M NaNO$_3$)	65.9	92.0	7
10Cu/TiO$_{2-x}$	0.5 M Na$_2$SO$_4$ (200 ppm NaNO$_3$)	114.3	81.3	8
Cu/TiO$_2$	0.5 M Na$_2$SO$_4$ (200 ppm NaNO$_3$)	/	88.1	9
P25-600	0.5 M Na$_2$SO$_4$ (100 ppm NaNO$_3$)	104.0	78.0	10
Fe SAC	0.1 M K$_2$SO$_4$ (0.5 M KNO$_3$)	308.5	75.0	11
Fe^0/Fe$_3$O$_4$	1.0 M NaOH (20 mM NaNO$_2$)	/	87.6	12
Fe-Co$_3$O$_4$	0.1 M PBS (50 mM NaNO$_3$)	36.7	95.5	13
Fe-PPy SACs	0.1 M NaOH (0.1 M NaNO$_3$)	161.7	~100.0	14
Fe$_3$O$_4$/SS	0.1 M NaOH (0.1 M NaNO$_3$)	596.7	91.5	15
BCN@Ni	0.1 M KOH (0.1 M NO$_3^-$)	140.0	91.1	16
BCN-Cu	0.1 M KOH (100 mM NO$_3^-$)	110.0	98.2	17
BC$_2$N/Pd	1 M KOH (0.25 M NO$_3^-$)	100.0	97.4	18

References

1   D. Zhu, L. Zhang, R. E. Ruther and R. J. Hamers, *Nat. Mater.,* 2013, **12**, 836–841.

2   L. C. Green, D. A. Wagner, J. Glogowski, P. L. Skipper, J. S. Wishnok and S. R. Tannenbaum, *Anal. Biochem.,* 1982, **126**, 131–138.

3   G. W. Watt and J. D. Chrisp, *Anal. Chem.,* 1952, **24**, 2006–2008.

4   P. E. Blöchl, *Phys. Rev. B.* 1994, **50**, 17953–17979.

5   J.P. Perdew, K. Burke and M. Ernzerhof, *Phys. Rev. Lett.,* 1996, **77**, 3865–3868.

6   R. Jia, Y. Wang, C. Wang, Y. Ling, Y. Yu and B. Zhang, *ACS Catal.,* 2020, **10**, 3533–3540.

7   Y. Guo, R. Zhang, S. Zhang, Y. Zhao, Q. Yang, Z. Huang, B. Dong and C. Zhi, *Energy Environ. Sci.,* 2021, **14**, 3938–3944.

8   X. Zhang, C. Wang, Y. Guo, B. Zhang, Y. Wang and Y. Yu, *J. Mater. Chem. A,* 2022, **10**, 6448–6453.

9   Q. Song, S. Zhang, X. Hou, J. Li, L. Yang, X. Liu and M. Li, *J. Hazard. Mater.,* 2022, **438**, 129455.

10 Z. Wei, X. Niu, H. Yin, S. Yu and J. Li, *Appl. Catal. A,* 2022, **636**, 118596.

11 Z. Y. Wu, M. Karamad, X. Yong, Q. Huang, D. A. Cullen, P. Zhu, C. Xia, Q. Xiao, M. Shakouri, F. Y. Chen, J. Y. T. Kim, Y. Xia, K. Heck, Y. Hu, M. S. Wong, Q. Li, I. Gates, S. Siahrostami and H. Wang, *Nat. Commun.*, 2021, **12**, 2870.

12 Z. A. Jonoush, A. Rezaee and A. Ghaffarinejad, *J. Clean. Prod.*, 2020, **242**, 118569.

13 P. Wei, J. Liang, Q. Liu, L. Xie, X. Tong, Y. Ren, T. Li, Y. Luo, N. Li, B. Tang, A. M. Asiri, M. S. Hamdy, Q. Kong, Z. Wang and X. Sun, *J. Colloid Interface Sci.*, 2022, **615**, 636–642.

14 P. Li, Z. Jin, Z. Fang and G. Yu, *Energy Environ. Sci.,* 2021, **14**, 3522–3531.

15 X. Fan, L. Xie, J. Liang, Y. Ren, L. Zhang, L. Yue, T. Li, Y. Luo, N. Li, B. Tang, Y. Liu, S. Gao, A. A. Alshehri, Q. Liu, Q. Kong and X. Sun, *Nano Res.*, 2022, **15**, 3050–3055.

16 X. Zhao, Z. Zhu, Y. He, H. Zhang, X. Zhou, W. Hu, M. Li, S. Zhang, Y. Dong, X. Hu, A. V. Kuklin, G. V. Baryshnikov, H. Ågren, T. Wågberg and G. Hu, *Chem. Eng. J.*, 2022, **433**, 133190.

17 X. Zhao, X. Jia, Y. He, H. Zhang, X. Zhou, H. Zhang, S. Zhang, Y. Dong, X. Hu, A. V. Kuklin, G. V. Baryshnikov, H. Ågren and G. Hu, *Appl. Mater. Today*, 2021, **25**, 101206.

18 X. Li, X. Zhao, Y. Zhou, J. Hu, H. Zhang, X. Hu and G. Hu, *Appl. Surf. Sci.*, 2022, **584**, 152556.